Ophthalmol Ther (2023) 12:125–138
https://doi.org/10.1007/s40123-022-00591-y

ORIGINAL RESEARCH

Comparison of Two Scheimpflug Systems in the Measurements of Eyes with Corneal Diameter Smaller than 11.1 mm

Lingling Niu · Lan Ding · Yishan Qian · Xingtao Zhou

Received: August 31, 2022 / Accepted: October 4, 2022 / Published online: October 16, 2022

ABSTRACT

Introduction: This article aimed to evaluate the measurements of ectasia parameters by two Scheimpflug-based tomography devices, Pentacam and Sirius, for eyes with different corneal diameters (CDs).

Methods: This cross-sectional research included subjects from the Fudan University EENT Hospital Refractive Center Database that were followed once a year for at least 3 years with unremarkable slit-lamp examination and normal topography. Pentacam and Sirius examinations were performed on these subjects and the ectasia indices were compared between different CD groups.

Results: The right eyes of 153 subjects were included (CD $\leq$ 11.1 mm, n = 50; 11.2–12 mm, n = 52; $>$ 12.0 mm, n = 51). For the ectasia parameters from Pentacam, CD had the greatest influence on the deviation of normality of back elevation (Db, $R^2 = 0.371$, $\beta = -1.119$, $P < 0.001$), overall deviation of normality (BAD-D, $R^2 = 0.305$, $\beta = -0.589$, $P < 0.001$), and minimum pachymetric progression index (PPI-min, $R^2 = 0.282$, $\beta = -0.131$, $P < 0.001$). For parameters derived from Sirius, CD had the greatest influence on Baiocchi–Calossi–Versaci index of the back surface (BCVb, $R^2 = 0.138$, $\beta = -0.179$, $P < 0.001$), keratoconus vertex of the back surface (KVb, $R^2 = 0.099$, $\beta = -2.273$, $P < 0.001$), and BCV ($R^2 = 0.071$, $\beta = -0.078$, $P = 0.001$). CD had little influence on surface asymmetry index of the front (SIf) and back surface (SIb), keratoconus vertex of the front surface (KVf), Baiocchi–Calossi–Versaci index of the front surface (BCVf), and Sirius classifier ($P > 0.05$).

Conclusions: For Pentacam, CD mainly influenced indices related to back elevation (BE) and pachymetry progression, whereas for Sirius, CD mainly influenced indices related to BE and corneal aberration.

Keywords: Scheimpflug; Tomography; Corneal diameter; Forme fruste keratoconus

Lingling Niu and Lan Ding contributed equally to this work and should be considered as equal first authors.

L. Niu · L. Ding · Y. Qian (✉) · X. Zhou (✉)
Department of Ophthalmology, Eye and ENT Hospital, NHC Key Laboratory of Myopia, Fudan University, Shanghai, People's Republic of China
e-mail: 13917852240@163.com

X. Zhou
e-mail: doctzhouxingtao@163.com

L. Niu
e-mail: niu-lingling@hotmail.com

L. Ding
e-mail: 158087780@qq.com

Key Summary Points

Why carry out this study?

Several studies have found that CD could influence the measurements of keratoconus parameters derived from the Pentacam tomography system. The Sirius tomography system combines two mechanisms of action, the Scheimpflug rotating camera and Placido disk topography. However, none of the previous studies have investigated the influence of CD on the performance of the Sirius tomography system.

What was learned from the study?

For Pentacam, CD mainly influenced indices related to back elevation (BE) and pachymetry progression, whereas for Sirius, CD mainly influenced indices related to BE and corneal aberration. The results of the two devices should be integrated as a reference in screening candidates for refractive surgery, especially for those with CD less than 11.1 mm.

INTRODUCTION

Scheimpflug tomography has become a widely employed technique in the early diagnosis of corneal ectasia. As reported previously, Chinese patients have a smaller corneal diameter (CD) than White patients [1]. Several studies have found that CD could influence the measurements of keratoconus parameters derived from the Pentacam tomography system (Oculus Optikgeraete GmbH; Wetzlar, Germany), including the Belin/Ambrósio Enhanced Ectasia Display (BAD) [2–4]. A previous study explored the performance of these descriptors in tomographically normal Chinese participants with different CDs and found that CD influences the BAD parameters, especially the deviation of normality of the back elevation (Db), back corneal elevation (BE), overall deviation of normality (BAD-D), and the minimum pachymetric progression indices (PPImin) [3]. The rates of suspected or abnormal cases were significantly higher in eyes with CD < 11 mm and lower in eyes with CD ≥ 12 mm. In a retrospective study with a large sample of Chinese patients ($n = 6744$), Cao et al. [4] also found that the false-positive rate of the BAD was higher in eyes with CD ≤ 11.1 mm. This was ascribed to the higher rate of change in the corneal curvature and thickness in smaller diameters. For the topometric indices related to the anterior surface of the cornea, Cao et al. found that the index of surface variance (ISV) and index of height asymmetry (IHA) were significantly higher in eyes with CD ≤ 11.1 mm, indicating a less regular surface in small cornea.

The Sirius tomography system (Costruzione Strumenti Oftalmici, Florence, Italy) combines two mechanisms of action, the Scheimpflug rotating camera and Placido disk topography. Data extrapolated from the Scheimpflug and Placido images were combined to deliver a surface tailored to the anterior surface of the cornea. Data from the posterior corneal surface were measured using edge detection in images provided by the Scheimpflug system. Several publications have compared the measurements of corneal indices between Pentacam and Sirius [5–11]. However, to our knowledge, none of the previous studies have investigated the influence of CD on the performance of the Sirius tomography system. In this study, we aimed to compare the measurements of ectasia parameters between Pentacam and Sirius in eyes with different horizontal CD.

METHODS

Subjects

This cross-section study included participants who were selected from the Fudan University EENT Hospital Refractive Center Database from January 2017 to January 2022. The inclusion criteria were as follows: participants who were followed up once a year for at least 3 years; age between 18 and 50 years; unremarkable slit-lamp examination; normal topography as

Table 1 Suggested cutoff values for keratoconus indices

	Abnormal
Pentacam	
ISV	≥ 37
IVA	≥ 0.28
KI	> 1.07
IHD	≥ 0.014
FE at TP	≥ 5.01
BE at TP	≥ 11.77
PPImin	≥ 0.79
PPIavg	≥ 1.15
PPImax	≥ 1.44
ARTmax	≤ 313
Sirius	
SIf (D)	≥ 0.85
SIb (D)	≥ 0.22
KVf (μm)	≥ 15
KVb (μm)	≥ 15
BCVf (μm)	≥ 0.58
BCVb (μm)	≥ 0.67
BCV (μm)	≥ 0.80

ISV index of surface variance, *IVA* index of vertical asymmetry, *KI* keratoconus index, *IHD* index of height decentration, *FE and BE at TP* front and back corneal elevations at thinnest pachymetry, *PPI* pachymetric progression index (minimum, average, and maximum), *ARTmax* Ambrosio's maximum relational thickness index, *SIf* surface asymmetry index of front surface, *Sib* surface asymmetry index of back surface, *KVf* keratoconus vertex front, *KVb* keratoconus vertex back, *BCVf* Baiocchi–Calossi–Versaci index for front surface, *BCVb* Baiocchi–Calossi–Versaci index for back surface, *BCV* vector summation of both surfaces

measured by Placido-disk corneal topography (TMS-5; Tomey; Aichi, Japan). A normal topography was defined as those without topographic signs of keratoconus according to both keratoconus screening programs (i.e., Klyce/Maeda Keratoconus Index and Smolek/Klyce Keratoconus Severity Index) and an inferior-superior asymmetry value (I-S value) of less than 1.4 diopters [12]. Those cases with any pathological ocular conditions or relevant systemic diseases or any previous ocular procedures (e.g., refractive surgery, corneal cross-linking, or intracorneal ring segments implantation) were excluded.

The selected patients were asked to come back and undergo a comprehensive ophthalmic examination, including slit-lamp examination, objective and subjective refractions, and Pentacam HR (version 1.21r43) and Sirius tomography system examinations (version 3.7). Soft contact lens usage was discontinued for at least 7 days before the examination, whereas rigid/hybrid contact lens usage was discontinued for a minimum period of 3 weeks. Only results from the current examination were used for statistics. The study participants were grouped according to their horizontal corneal diameter measured by Pentacam. A previous study found that the mean CD in Chinese adult was 11.66 ± 0.38 mm [4]. Therefore, we set the cutoffs of CD as small (≤ 11.1 mm), medium (11.2–12.0 mm), and large (> 12.0 mm).

This study was approved by the Ethics Committee of the Eye and ENT Hospital of Fudan University (Shanghai, China), and was conducted in compliance with the tenets of the Declaration of Helsinki. Written informed consent was obtained from all participants.

Corneal Tomography

One experienced examiner performed Pentacam imaging and another examiner performed Sirius imaging for all participants (three measurements were averaged for each individual). Only scans registered as "OK" by the examination quality specification of the instrument were recorded and analyzed. All the analyzing dimensions for both devices were 8 mm in diameter.

Both pieces of software obtained the following corneal descriptors: horizontal corneal diameter; mean central powers for the front and back in a 3.0-mm zone of the cornea (Km_f and

Table 2 Means, ranges and results of paired t test for readings taken by two devices

	≤ 11.1 mm (*n* = 50)				11.2–12.0 mm (*n* = 52)			
	Pentacam	**Sirius**	**Mean difference**	***P***	**Pentacam**	**Sirius**	**Mean difference**	***P***
CD (mm)	10.91 ± 0.18 (10.40, 11.10)	10.71 ± 0.19 (10.30, 11.10)	0.20 ± 0.12 (− 0.25, 0.39)	< 0.001	11.59 ± 0.21 (11.20, 12.00)	11.40 ± 0.23 (11.00, 12.09)	0.20 ± 0.12 (− 0.14, 0.44)	< 0.001
TP (μm)	539.1 ± 29.3 (488, 611)	539.1 ± 31.1 (488, 612)	0.02 ± 5.7 (− 15, 8)	0.98	531.3 ± 24.5 (485, 585)	529.9 ± 25.8 (488, 603)	1.42 ± 7.40 (− 25, 12)	0.124
Km_f (D)	44.53 ± 1.52 (41.35, 47.05)	44.86 ± 1.53 (41.67, 47.40)	− 0.32 ± 0.19 (− 1.30, − 0.02)	< 0.001	42.98 ± 1.33 (39.30, 45.50)	43.28 ± 1.33 (39.63, 45.76)	− 0.30 ± 0.19 (− 1.19, 0.11)	< 0.001
Ka_f (D)	1.15 ± 0.95 (0.00, 4.30)	1.12 ± 0.97 (0.09, 4.51)	0.03 ± 0.17 (− 0.50, 0.55)	0.222	1.11 ± 0.71 (0.00, 2.90)	1.05 ± 0.67 (0.14, 2.73)	0.06 ± 0.32 (− 1.93, 0.68)	0.102
Km_b (D)	− 6.58 ± 0.25 (− 7.10, − 6.05)	-6.45 ± 0.24 (− 7.00, − 5.90)	− 0.13 ± 0.07 (− 0.46, − 0.04)	< 0.001	− 6.28 ± 0.23 (− 6.75, − 5.85)	− 6.17 ± 0.23 (− 6.65, − 5.69)	− 0.11 ± 0.04 (− 0.23, 0.01)	< 0.001
Ka_b (D)	0.32 ± 0.17 (0.10, 0.80)	0.40 ± 0.17 (0.12, 1.00)	− 0.08 ± 0.08 (− 0.22, 0.11)	< 0.001	0.34 ± 0.16 (0.00, 0.70)	0.41 ± 0.16 (0.08, 0.78)	− 0.07 ± 0.07 (− 0.20, 0.12)	< 0.001
BFS_f (mm)	7.68 ± 0.26 (7.20, 8.25)	7.61 ± 0.26 (7.14, 8.16)	0.07 ± 0.03 (0.03, 0.19)	< 0.001	7.96 ± 0.25 (7.51, 8.66)	7.88 ± 0.25 (7.43, 8.57)	0.08 ± 0.02 (0.04, 0.12)	< 0.001
BFS_b (mm)	6.22 ± 0.23 (5.85, 6.70)	6.31 ± 0.23 (5.97, 6.87)	− 0.10 ± 0.04 (-0.17, − 0.03)	< 0.001	6.46 ± 0.23 (5.99, 6.87)	6.57 ± 0.23 (6.18, 7.01)	− 0.11 ± 0.04 (− 0.19, − 0.01)	< 0.001
FE at TP (μm)	2.18 ± 1.34 (0, 5)	0.76 ± 0.63 (− 1, 2)	1.42 ± 1.13 (0, 4)	< 0.001	2.62 ± 1.29 (− 1, 5)	1.04 ± 0.77 (− 1, 2)	1.58 ± 1.04 (− 1, 4)	< 0.001
BE at TP (μm)	6.90 ± 4.74 (0, 22)	2.84 ± 2.17 (0, 11)	4.06 ± 3.68 (− 2, 12)	< 0.001	5.19 ± 3.75 (− 1, 14)	1.94 ± 2.13 (− 3, 9)	3.25 ± 2.68 (− 2, 9)	< 0.001
ACD (mm)	2.98 ± 0.18 (2.63, 3.33)	3.02 ± 0.20 (2.61, 3.43)	− 0.03 ± 0.05 (− 0.14, 0.04)	< 0.001	3.09 ± 0.27 (2.40, 3.59)	3.14 ± 0.24 (2.63, 3.63)	− 0.05 ± 0.10 (− 0.55, 0.11)	< 0.001

	> 12.0 mm (*n* = 51)			
	Pentacam	**Sirius**	**Mean difference**	***P***
CD (mm)	12.38 ± 0.17 (12.20, 12.80)	12.21 ± 0.15 (11.95, 12.63)	0.17 ± 0.08 (− 0.03, 0.35)	< 0.001
TP (μm)	529.6 ± 20.5 (481, 574)	527.2 ± 22.1 (480, 570)	2.31 ± 6.41 (− 11, 18)	0.013
Km_f (D)	42.24 ± 1.08 (39.95, 44.35)	42.51 ± 1.05 (40.28, 44.75)	− 0.27 ± 0.15 (− 0.75, 0.12)	< 0.001

Table 2 continued

	> 12.0 mm (n = 51)			
	Pentacam	**Sirius**	**Mean difference**	***P***
Ka_f (D)	1.50 ± 0.61 (0.40, 2.80)	1.41 ± 0.61 (0.49, 2.82)	0.09 ± 0.19 (− 0.52, 0.70)	0.001
Km_b (D)	− 6.05 ± 0.17 (− 6.45, − 5.70)	− 5.94 ± 0.18 (-6.35, − 5.56)	− 0.11 ± 0.08 (− 0.20, 0.35)	< 0.001
Ka_b (D)	0.40 ± 0.12 (0.20, 0.70)	0.49 ± 0.13 (0.23, 0.81)	− 0.09 ± 0.08 (− 0.25, 0.12)	< 0.001
BFS_f (mm)	8.09 ± 0.21 (7.71, 8.55)	8.00 ± 0.20 (7.63, 8.44)	0.09 ± 0.03 (− 0.01, 0.15)	< 0.001
BFS_b (mm)	6.64 ± 0.17 (6.29, 6.92)	6.78 ± 0.18 (6.41, 7.06)	− 0.13 ± 0.04 (− 0.23, − 0.05)	< 0.001
FE at TP (µm)	2.67 ± 1.13 (− 1, 5)	1.02 ± 1.61 (-2, 8)	1.65 ± 1.67 (− 4.97, 4)	< 0.001
BE at TP (µm)	3.69 ± 3.08 (− 4, 14)	1.21 ± 2.41 (− 2, 7)	2.48 ± 2.56 (-2, 9)	< 0.001
ACD (mm)	3.37 ± 0.23 (2.92, 3.86)	3.39 ± 0.22 (2.99, 3.93)	− 0.02 ± 0.05 (-0.15, 0.05)	0.004

CD corneal diameter, *TP* thinnest pachymetry, *Km_f and Km_b* mean central power for the front and back surface, *Ka_f and Ka_b* corneal astigmatism for the front and back surface, *BFS_f and BFS_b* best fit sphere for the front and back cornea, *FE and BE at TP* front and back corneal elevations at thinnest pachymetry; *ACD* anterior chamber depth

Km_b, respectively); corneal astigmatism for the front and back in a 3.0-mm zone (Ka_f and Ka_b, respectively); the best-fit sphere for the front and back cornea which were automatically generated by the devices (BFS_f and BFS_b for Pentacam and $sBFS_f$ and $sBFS_b$ for Sirius, respectively); thinnest pachymetry (TP); front and back corneal elevations at TP (FE and BE for Pentacam and sFE and sBE for Sirius, respectively); anterior chamber depth (ACD). The majority of the metrics were exported automatically, except for the sFE and sBE in Sirius which were collected manually from the elevation maps.

In Pentacam, the following keratoconus summary descriptors were investigated: index of surface variance (ISV), index of vertical asymmetry (IVA), keratoconus index (KI), index of height decentration (IHD), pachymetric progression index (PPI; minimum, average, and maximum), and Ambrósio's maximum relational thickness index (ARTmax). The BAD normalized indices include deviation of normality of the front elevation (Df), deviation of normality of the back elevation (Db), deviation of normality of pachymetric progression (Dp), deviation of normality of the thinnest corneal point (Dt), deviation of normality of relational thickness (Da), and overall deviation of normality (BAD-D). The deviation-based indices could be classified by the software as normal (< 1.6 standard deviations [SD] from the population mean, white), suspected (> 1.6 and < 2.6 SD, yellow), and pathological (> 2.6 SD, red). In Sirius, the following keratoconus summary descriptors were investigated: keratoconus vertex of the front (KVf) and back surfaces (KVb); surface asymmetry index of the front (SIf) and back surfaces (SIb); Baiocchi–Calossi–Versaci index of the front (BCVf) and back surfaces (BCVb); vector summation of both surfaces (BCV), and the keratoconus classifier based on the support vector machine. The suggested cutoff values for the aforementioned indices as reported by the manufacturer [13, 14] are listed in Table 1. For the convenience of statistics, eyes classified as "suspected" and "pathological" were combined as "abnormal".

Table 3 Regression analyses for individual keratoconus descriptors for two devices with respect to corneal diameter

	Unstandardized β	R^2	P
Pentacam			
ISV	0.598	0.006	0.329
IVA	0.008	0.020	0.079
KI	− 0.032	0.020	0.08
IHD	0.000	0.006	0.36
BFS_f	0.286	0.358	< 0.001
BFS_b	0.291	0.441	< 0.001
FE at TP	0.290	0.021	0.077
BE at TP	− 2.305	0.124	< 0.001
Df	− 0.316	0.052	0.005
Db	− 1.119	0.371	< 0.001
Dp	− 0.770	0.228	< 0.001
Dt	0.147	0.016	0.115
Da	− 0.212	0.040	0.013
BAD-D	− 0.589	0.305	< 0.001
PPImin	− 0.131	0.282	< 0.001
PPIavg	− 0.121	0.172	< 0.001
PPImax	− 0.055	0.025	0.05
ARTmax	22.748	0.038	0.016
Sirius			
$sBFS_f$	0.264	0.347	< 0.001
$sBFS_b$	0.308	0.477	< 0.001
sFE at TP	0.132	0.006	0.343
sBE at TP	− 1.075	0.088	< 0.001
SIf (D)	0.018	0.001	0.745
SIb (D)	0.015	0.007	0.319
KVf (μm)	− 0.152	0.007	0.316
KVb (μm)	− 2.273	0.099	< 0.001
BCVf (μm)	− 0.008	0.001	0.722
BCVb (μm)	− 0.179	0.138	< 0.001
BCV (μm)	− 0.078	0.071	0.001

ISV index of surface variance, *IVA* index of vertical asymmetry, *KI* keratoconus index, *IHD* index of height decentration, *BFSf and BFSb* best fit sphere for the front and back surface, *FE and BE at TP* front and back corneal elevations at thinnest pachymetry, *Df* deviation of normality of the front elevation, *Db* deviation of normality of the back elevation, *DP* deviation of normality of pachymetric progression, *Dt* deviation of normality of corneal thinnest point, *Da* deviation of normality of relational thickness, *BAD-D* overall deviation of normality, *PPI* pachymetric progression index (minimum, average, and maximum), *ARTmax* Ambrosio's maximum relational thickness index, *sBFSf and sBFSb* best fit sphere for the front and back surface in Sirius, *sFE and sBE at TP* front and back corneal elevations at thinnest pachymetry in Sirius, *SIf* surface asymmetry index of front surface, *Sib* surface asymmetry index of back surface, *KVf* keratoconus vertex front, *KVb* keratoconus vertex back, *BCVf* Baiocchi–Calossi–Versaci index for front surface, *BCVb* Baiocchi–Calossi–Versaci index for back surface, *BCV* vector summation of both surfaces

Statistical Analysis

Statistical analysis was performed using SPSS (v. 23.0, IBM Corp, Armonk, NY, USA). Comparisons for individual corneal descriptors between two devices were carried out using paired *t* test. Comparisons between CD groups were carried out using one-way analysis of variance (ANOVA). Linear regression analyses were performed for indices with respect to CD. The percentages of abnormality between groups were compared by chi-squared test. $P < 0.05$ was considered statistically significant.

RESULTS

The right eyes of 72 men (47.1%) and 81 women (52.9%) were included. The number in each CD group was as follows: 11.1 mm or less, $n = 50$; 11.2–12 mm, $n = 52$; and 12.1 mm or greater, $n = 51$. The mean age was 27.9 ± 5.1 years for the CD ≤ 11.1 group,

26.6 ± 6.5 years for the CD 11.2–12.0 group, and 26.0 ± 5.3 years for the CD > 12.0 mm group (ANOVA: $F = 0.721$, $P = 0.489$). The mean of the spherical error at the spectacle plane was − 3.98 ± 2.06 D (range − 1.0 to − 10.0 D) for the CD ≤ 11.1 group, − 4.17 ± 2.06 D (range − 1.0 to − 9.0 D) for the CD 11.2–12.0 group, and − 3.53 ± 1.45 D (range − 1.0 to − 8.0 D) for the CD > 12.0 mm group (ANOVA: $F = 1.593$, $P = 0.207$). The mean of the cylindrical error at the spectacle plane was − 1.15 ± 0.95 D (range − 3.5 to 0 D) for the CD ≤ 11.1 group, − 1.11 ± 0.71 D (range − 3.0 to 0 D) for the CD 11.2–12.0 group, and − 1.50 ± 0.61 D (range − 3.0 to 0 D) for the CD > 12.0 mm group (ANOVA: $F = 3.909$, $P = 0.022$).

Table 2 summarizes the means and results of paired *t* test for readings taken by two devices. The results of regression analyses for individual keratoconus descriptors with respect to CD are shown in Table 3. For parameters derived from Pentacam, BFS_f, BFS_b, and ARTmax were positively correlated with CD, while BE, Df, Db, Dp, Da, BAD-D, PPImin, and PPIavg were negatively correlated with CD ($P < 0.05$). CD had the greatest influence on BFS_b ($R^2 = 0.441$, $\beta = 0.291$, $P < 0.001$), then on Db ($R^2 = 0.371$, $\beta = -1.119$, $P < 0.001$), BFS_f ($R^2 = 0.358$, $\beta = 0.286$, $P < 0.001$), BAD-D ($R^2 = 0.305$, $\beta = -0.589$, $P < 0.001$), and PPImin ($R^2 = 0.282$, $\beta = -0.131$, $P < 0.001$). CD had little influence on the four topometric indices (ISV, IVA, KI, IHD), FE, Dt, and PPImax ($P > 0.05$). The scatter plots for the indices of Pentacam with respect to CD (only parameters with $P < 0.05$) are displayed in Fig. 1

For parameters derived from Sirius, $sBFS_f$ and $sBFS_b$ were positively correlated with CD while sBE, KVb, BCVb, and BCV were negatively correlated with CD ($P < 0.05$). CD had the greatest influence on $sBFS_b$ ($R^2 = 0.477$, $\beta = 0.308$, $P < 0.001$), followed by $sBFS_f$ ($R^2 = 0.347$, $\beta = 0.264$, $P < 0.001$), BCVb ($R^2 = 0.138$, $\beta = -0.179$, $P < 0.001$), KVb ($R^2 = 0.099$, $\beta = -2.273$, $P < 0.001$), sBE ($R^2 = 0.088$, $\beta = -1.075$, $P = 0.001$), and BCV ($R^2 = 0.071$, $\beta = -0.078$, $P = 0.001$). CD had little influence on FE, SIf, SIb, KVf, BCVf, and Sirius classifier ($P > 0.05$). The scatter plots for the indices of Sirius with respect to CD (only parameters with $P < 0.05$) are displayed in Fig. 2.

Table 4 listed the results of classification for the keratoconus indices with respect to CD. For parameters derived from Pentacam, the differences in the classifications between the three CD groups were statistically significant (Pearson's chi-square test, $P < 0.05$) for the following indices: BE, Df, Db, Dp, BAD-D, PPImin, and PPIavg. For parameters derived from Sirius, the difference in the classifications between the three CD groups was significant for KVb (Pearson's chi-square test, $P = 0.003$).

Overall, the numbers and percentages of eyes with normal values for all the 10 indices of Pentacam (four PPIs plus six BAD indices) were 5 (10%), 15 (26.3%), and 34 (66.7%) for the three CD groups, respectively. The numbers and percentages of eyes with normal values for all the eight indices of Sirius (SIf, SIb, KVf, KVb, BCVf, BCVb, BCV, and Sirius classifier) were 21 (42%), 31 (59.6%), and 31 (60.8%) for the three groups, respectively.

DISCUSSION

To date, few studies have focused on the influence of CD on the performance of Sirius [15]. In this study, we evaluated the performance of the Sirius system in participants with different CDs and compared it with that of Pentacam HR. The correlations between CDs and BAD indices in Pentacam were consistent with previous publications [2–4]. What is added in the current study is that CD also influenced indices of Sirius, e.g., $sBFS_b$, $sBFS_f$, KVb, BCVb, and BCV, but the difference in the classifications for the keratoconus indices between three CD groups was significant only for KVb.

Best fit sphere (BFS) is the standardized reference shape that is calculated on the basis of the value of the central and eccentric radii of cornea. In corneas with a small diameter, both the BFS_f and BFS_b may have an increased radius of curvature (flatter power) because the curvature may become flat earlier in small diameter, leading to an increased elevation above the standardized reference shape. Meanwhile, KVb is the maximum elevation of the posterior

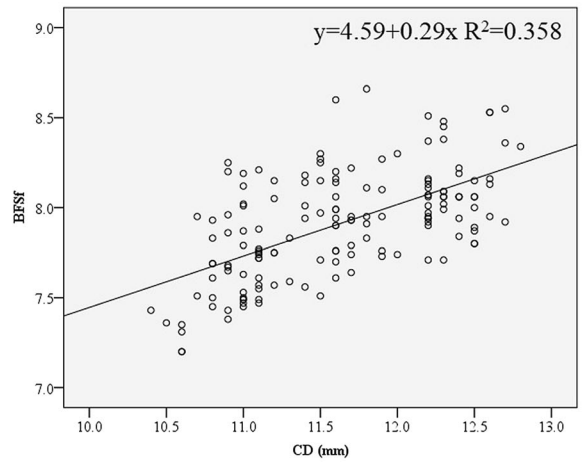
y=4.59+0.29x R²=0.358
BFSf
CD (mm)

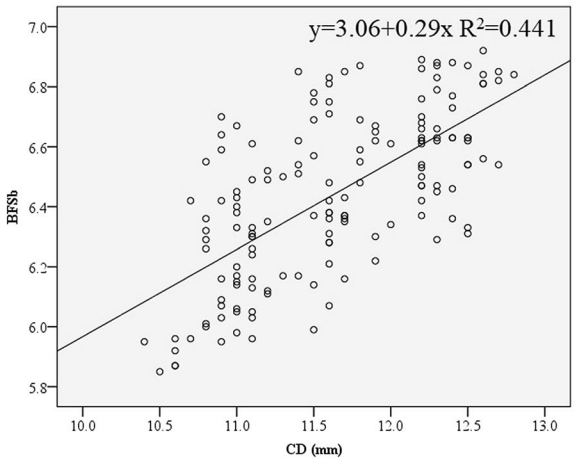
y=3.06+0.29x R²=0.441
BFSb
CD (mm)

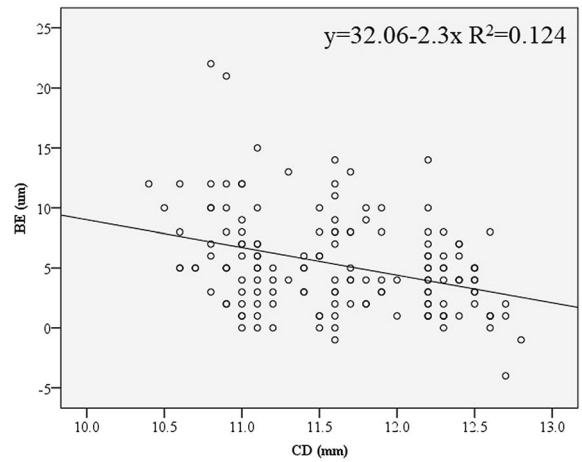
y=32.06-2.3x R²=0.124
BE (um)
CD (mm)

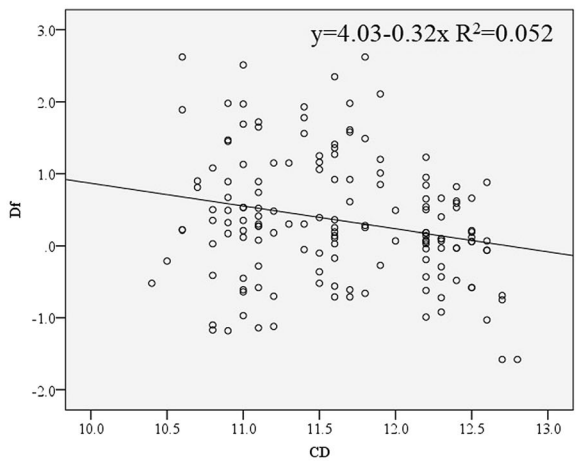
y=4.03-0.32x R²=0.052
Df
CD

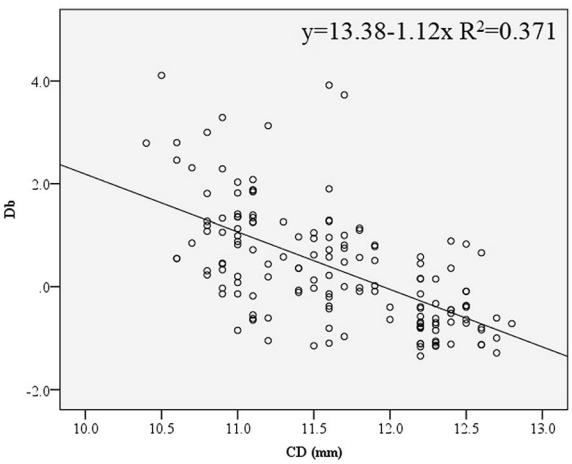
y=13.38-1.12x R²=0.371
Db
CD (mm)

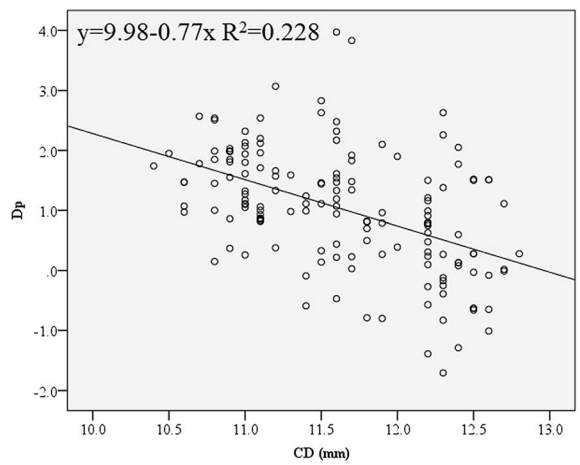
y=9.98-0.77x R²=0.228
Dp
CD (mm)

◀**Fig. 1** Scatter plots for the indices of Pentacam with respect to corneal diameter. *BFSf and BFSb* best fit sphere for the front and back surface, *BE* back corneal elevation at thinnest pachymetry, *Df* deviation of normality of the front elevation, *Db* deviation of normality of the back elevation, *DP* deviation of normality of pachymetric progression, *BAD-D* overall deviation of normality, *PPI* pachymetric progression index (minimum, average), *ART-max* Ambrosio's maximum relational thickness index

cornea (height of posterior vertex). It is the counterpart of BE at TP in Pentacam. But it is not equal to BE at TP which represents the elevation of the posterior cornea at the thinnest point. The possible explanation for the greater influence of CD on BE than on FE is that the posterior cornea may become flat more quickly than the anterior cornea toward the limbus in small cornea because the curvature is steeper in the posterior cornea [3]. BCVb is obtained by combining different aberration coefficients, including vertical trefoil, vertical coma, horizontal coma, spherical aberration (SA), and second-order vertical coma from the posterior corneal surface, and BCV is the vector summation of both surfaces. BCV index has been proved to show great accuracy in diagnosing keratoconus with great sensitivity and specificity in previous publications [9, 14]. The higher BCVb and BCV could be related to the steeper curvature [16] and shallower ACD [17] in small cornea. Previous studies have found that the corneal spherical aberration became more positive with increasing power of the corneal surface [16]. Davis et al. [18] ascribed

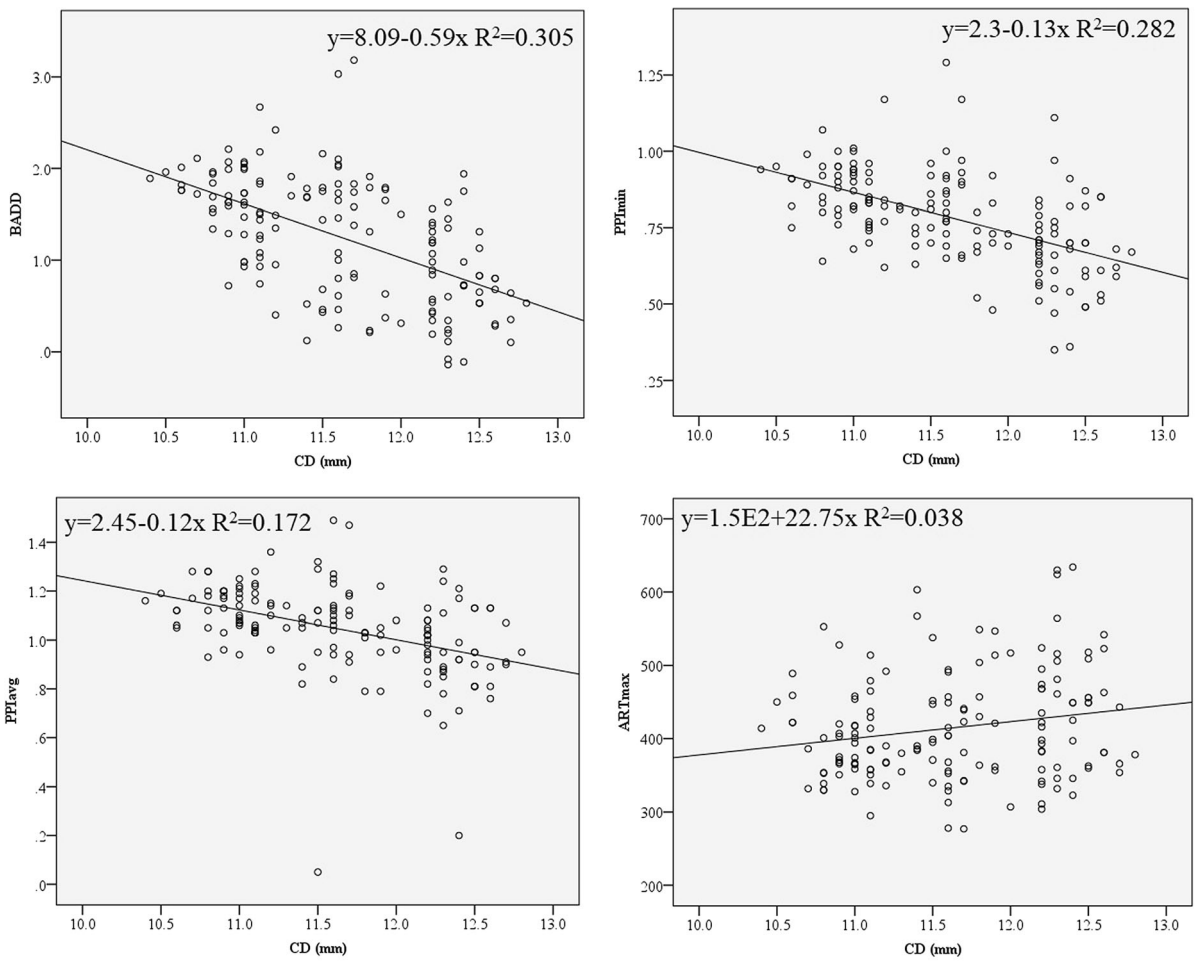

Fig. 1 continued

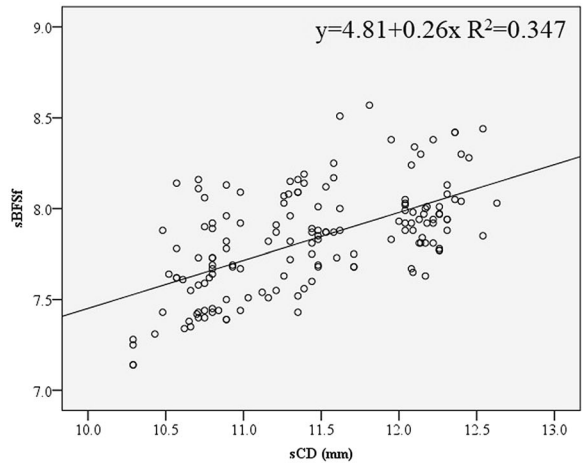
y=4.81+0.26x R²=0.347
sBFSf
sCD (mm)

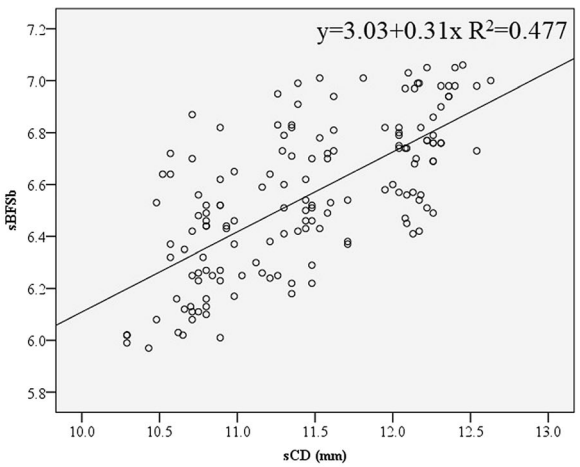
y=3.03+0.31x R²=0.477
sBFSb
sCD (mm)

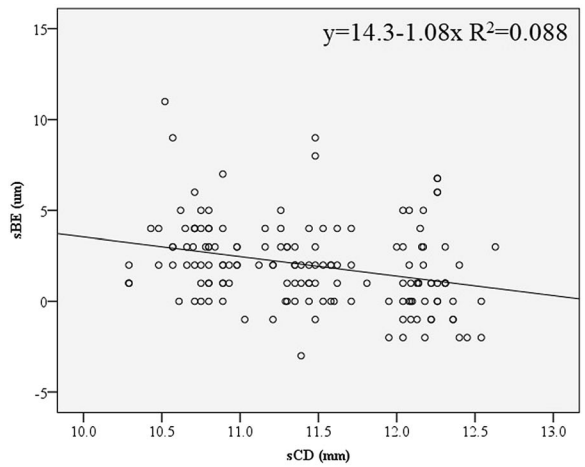
y=14.3-1.08x R²=0.088
sBE (um)
sCD (mm)

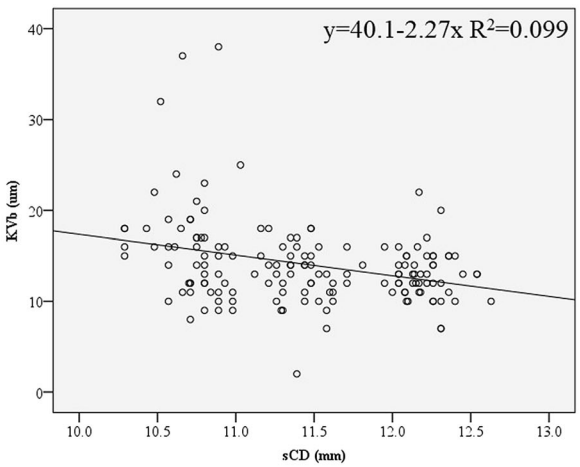
y=40.1-2.27x R²=0.099
KVb (um)
sCD (mm)

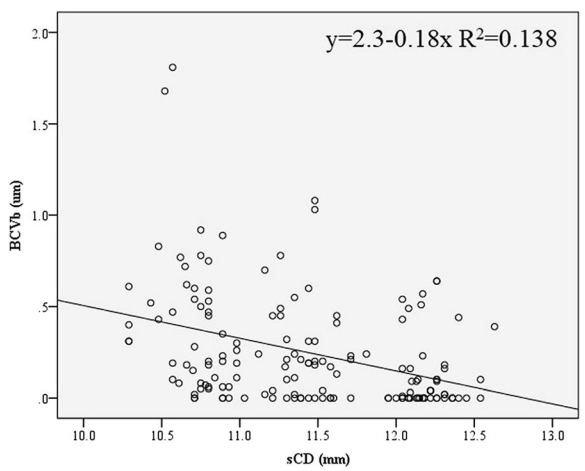
y=2.3-0.18x R²=0.138
BCVb (um)
sCD (mm)

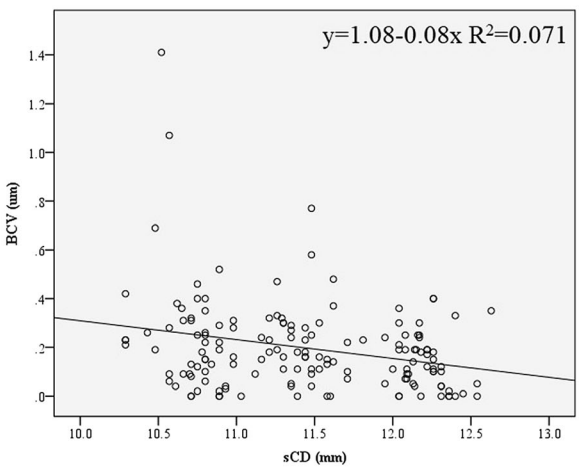
y=1.08-0.08x R²=0.071
BCV (um)
sCD (mm)

◀**Fig. 2** Scatter plots for the indices of Sirius with respect to corneal diameter. *sBFSf and sBFSb* best fit sphere for the front and back surface in Sirius, *sBE* back corneal elevations at thinnest pachymetry in Sirius, *KVb* keratoconus vertex back, *BCVb* Baiocchi–Calossi–Versaci index for back surface, *BCV* vector summation of both surfaces

the correlation between ACD and corneal asphericity to the mechanical influences on the peripheral cornea as the anterior chamber elongates during ocular growth. Further study is needed to explore the profile of aberrations in regard to corneal diameters, which may help to determine the individualized analytical dimension for each CD.

This study found that CD had no correlation with the following indices: KVf, SIf, and SIb. KVf is the maximum elevation of the anterior cornea (height of anterior vertex). Similarly, no correlation was found between FE and CD in Pentacam. Surface asymmetry index is defined as the difference of the mean tangential curvature (expressed in diopters) of two circular zones centered on the vertical axis of the inferior and superior hemispheres of front surface (SIf) and back surface (SIb). Likewise, we found no correlation between CD and the four topometric indices in Pentacam. In contrast, Cao et al. found higher ISV and IHA in eyes with CD less than 11.1 mm. The possible explanation for the discrepancy is that only patients with normal topography (i.e., Klyce/Maeda Keratoconus Index = 0; Smolek/Klyce Keratoconus Severity Index = 0; and I–S value $\leq$ 1.4 D) were included in the study.

Both BAD-D and Sirius classifier are multivariate indices that combined several key indicators of ectasia. The BAD-D derived from Pentacam is an integrated index that considers nine separate screenings for subclinical keratoconus. BAD-D has been shown in multiple studies to have a high accuracy in detecting both clinical and subclinical keratoconus [18, 19]. In the current study we found that the rates of being flagged as abnormal cases for BAD-D were 60% for CD $\leq$ 11.1 mm, 46.2% for CD 11.2–12.0 mm, and 5.9% for CD > 12.0 mm. The significant differences in the rate of abnormality between different CD-based groups indicate that corneal diameter should be incorporated as additional parameter for BAD-D. Meanwhile, the Sirius classifier is provided by support vector machine. It integrates indices obtained from the anterior and posterior corneas and corneal thickness. In the current study we found that the rates of being flagged as abnormal cases for the Sirius classifier were 6.0% for CD $\leq$ 11.1 mm, 5.8% for CD 11.2–12.0 mm, and 7.8% for CD > 12.0 mm. It seems that CD has little influence on the Sirius classifier. Previous publications regarding the Sirius classifier are limited. Arbelaez et al. [20] showed that the accuracy of the classifier was excellent, and the sensitivity and specificity in distinguishing eyes with subclinical keratoconus from normal eyes were 92.0% and 97.7%, respectively. Therefore, the difference in the performances between BAD-D and the Sirius classifier could not be ascribed to the difference in the accuracy and sensitivity between them. Further studies are needed to evaluate the performance of the Sirius classifier in subclinical keratoconus with different CDs.

The main limitation of the study is that the inclusion criteria were based only on the topography system. It is possible that forme fruste keratoconus (FFKC) eyes may remain normal in topography measurements. In order to reduce errors brought by the inclusion criteria, we included only patients who were followed up for at least 3 years and their topographies remained normal. According to the recently published Global Consensus on Keratoconus and Ectatic Diseases [21], there is currently no clinically adequate classification system for keratoconus. Further study using a third tomography device, e.g., the Orbscan topography system (Bausch & Lomb, Orbtek Inc., Utah, USA) or the Galilei dual Scheimpflug system (Ziemer Ophthalmic Systems AG, Port, Switzerland) along with biomechanical assessment of cornea would give additional information in this field [22]. The second limitation is that only eyes labelled as normal were included in the study, further research is needed to investigate the issue in a population of suspect keratoconus with different corneal diameters.

Table 4 Results of classification for individual keratoconus indices for the two devices

	≤ 11.1 mm (*n* = 50)		11.2–12.0 mm (*n* = 52)		> 12.0 mm (*n* = 51)		Chi-square	*P*
	Normal	Abnormal	Normal	Abnormal	Normal	Abnormal		
Pentacam								
ISV	50 (100%)	0 (0%)	52 (100%)	0 (0%)	51 (100%)	0 (0%)	NA	NA
IVA	50 (100%)	0 (0%)	52 (100%)	0 (0%)	51 (100%)	0 (0%)	NA	NA
KI	50 (100%)	0 (0%)	50 (96.2%)	2 (3.8%)	50 (98%)	1 (2%)	NA	NA
IHD	50 (100%)	0 (0%)	52 (100%)	0 (0%)	51 (100%)	0 (0%)	NA	NA
FE	50 (100%)	0 (0%)	52 (100%)	0 (0%)	51 (100%)	0 (0%)	NA	NA
BE	40 (80%)	10 (20%)	48 (92.3%)	4 (7.7%)	50 (98%)	1 (2%)	9.69	0.008
Df	42 (84%)	8 (16%)	45 (86.5%)	7 (13.5%)	51 (100%)	0 (0%)	8.50	0.014
Db	35 (70%)	15 (30%)	48 (92.3%)	4 (7.7%)	51 (100%)	0 (0%)	22.51	< 0.001
Dp	25 (50%)	25 (50%)	38 (73.1%)	14 (26.9%)	47 (92.2%)	4 (7.8%)	21.26	< 0.001
Dt	50 (100%)	0 (0%)	51 (98.1%)	1 (1.9%)	50 (98%)	1 (2%)	NA	NA
Da	49 (98%)	1 (2%)	47 (90.4%)	5 (9.6%)	49 (96.1%)	2 (3.9%)	NA	NA
BAD-D	20 (40%)	30 (60%)	28 (53.8%)	24 (46.2%)	48 (94.1%)	3 (5.9%)	34.30	< 0.001
PPImin	9 (18%)	41 (82%)	25 (48.1%)	27 (51.9%)	40 (78.4%)	11 (21.6%)	36.92	< 0.001
PPImax	33 (66%)	17 (34%)	37 (71.2%)	15 (28.8%)	39 (76.5%)	12 (23.5%)	1.35	0.509
PPIavg	26 (52%)	24 (48%)	40 (76.9%)	12 (23.1%)	47 (92.2%)	4 (7.8%)	21.47	< 0.001
ARTmax	49 (98%)	1 (2%)	48 (92.3%)	4 (7.7%)	49 (96.1%)	2 (3.9%)	NA	NA
Sirius								
SIf	49 (98%)	1 (2%)	52 (100%)	0 (0%)	49 (96.1%)	2 (3.9%)	NA	NA
SIb	48 (96%)	2 (4%)	43 (82.7%)	9 (17.3%)	44 (86.3%)	7 (13.7%)	4.63	0.099
KVf	50 (100%)	0 (0%)	52 (100%)	0 (0%)	50 (98%)	1 (2%)	NA	NA
KVb	21 (42%)	29 (58%)	36 (69.2%)	16 (30.8%)	37 (72.5%)	14 (27.5%)	11.96	0.003
BCVf	48 (96%)	2 (4%)	49 (94.2%)	3 (5.8%)	51 (100%)	0 (0%)	NA	NA
BCVb	41 (82%)	9 (18%)	48 (92.3%)	4 (7.7%)	51 (100%)	0 (0%)	NA	NA
BCV	48 (96%)	2 (4%)	52 (100%)	0 (0%)	51 (100%)	0 (0%)	NA	NA
Sirius classifier	47 (94%)	3 (6%)	49 (94.2%)	3 (5.8%)	47 (92.2%)	4 (7.8%)	NA	NA

ISV index of surface variance, *IVA* index of vertical asymmetry, *KI* keratoconus index, *IHD* index of height decentration, *FE and BE at TP* front and back corneal elevations at thinnest pachymetry, *Df* deviation of normality of the front elevation, *Db* deviation of normality of the back elevation, *DP* deviation of normality of pachymetric progression, *Dt* deviation of normality of corneal thinnest point, *Da* deviation of normality of relational thickness, *BAD-D* overall deviation of normality, *PPI* pachymetric progression index (minimum, average, and maximum), *ARTmax* Ambrosio's maximum relational thickness index, *SIf* surface asymmetry index of front surface, *Sib* surface asymmetry index of back surface, *KVf* keratoconus vertex front, *KVb* keratoconus vertex back, *BCVf* Baiocchi–Calossi–Versaci index for front surface, *BCVb* Baiocchi–Calossi–Versaci index for back surface, *BCV* vector summation of both surfaces

CONCLUSIONS

In this study, we found that for Pentacam, corneal diameter mainly influenced indices related to back elevation and pachymetry progression. For Sirius, CD mainly influenced indices related to back elevation and corneal aberration (e.g., KVb, BCVb, and BCV). For both devices, CD had little influence on parameters related to the shape symmetry of the cornea (e.g., topometric indices in Pentacam; SIf and SIb in Sirius). For the integrative indices, CD is highly correlated with BAD-D, but not with the Sirius classifier. The results of the two devices should be integrated as a reference in screening candidates for refractive surgery, especially for those with CD less than 11.1 mm.

ACKNOWLEDGEMENTS

Funding. The study, and the journal's Rapid Service Fee, was supported by the National Natural Science Foundation of China (grant no. 81770955) and Project of Shanghai Science and Technology (grant no.17411950200).

Authorship. All named authors meet the International Committee of Medical Journal Editors (ICMJE) criteria for authorship for this manuscript, take responsibility for the integrity of the work, and have given final approval to the version to be published.

Author Contributions. Conceptualization: Yishan Qian; Methodology: Lingling Niu and Lan Ding; Formal analysis and investigation: Lingling Niu and Lan Ding; Writing—original draft preparation: Yishan Qian; Writing—review and editing: Xingtao Zhou; Funding acquisition: Xingtao Zhou; Supervision: Xingtao Zhou.

Disclosures. Lingling Niu, Lan Ding, Yishan Qian and Xingtao Zhou declare that they have no actual or potential conflicts of interest related to this submission.

Compliance with Ethics Guidelines. Ethics approval for this study was granted by the Ethics Committee of the Eye and ENT Hospital of Fudan University (Shanghai, China. No. 0811/2021), and was conducted in compliance with the tenets of the Declaration of Helsinki.

Data Availability. The datasets generated during and/or analyzed during the current study are available from the corresponding author on reasonable request.

REFERENCES

1. Qin B, Tang M, Li Y, Zhang X, Chu R, Huang D. Anterior segment dimensions in Asian and Caucasian eyes measured by optical coherence tomography. Ophthalmic Surg Lasers Imaging. 2012;43(2):135–42.

2. Boyd BM, Bai J, Borgstrom M, Belin MW. Comparison of Chinese and North American tomographic parameters and the implications for refractive surgery screening. Asia Pac J Ophthalmol (Phila). 2020;9(2):117–25.

3. Ding L, Wang J, Niu L, Shi W, Qian Y. Pentacam Scheimpflug tomography findings in chinese patients with different corneal diameters. J Refract Surg. 2020;36(10):688–95.

4. Cao KW, Liu LN, Sun YL, Zhang T, Bai J, Liu T. The influence of different corneal diameters on Belin/Ambrósio enhanced ectasia display of Pentacam corneal topography. Zhonghua Yan Ke Za Zhi. 2020;56(10):761–7.

5. Nasser CK, Singer R, Barkana Y, et al. Repeatability of the Sirius imaging system and agreement with the Pentacam HR. J Refract Surg. 2012;28(7):493–7.

6. Gharieb HM, Shalaby HS, Othman IS. Repeatability and interchangeability of topometric, anterior chamber and corneal wavefront data between two Scheimpflug camera devices. Clin Ophthalmol. 2020;14:3801–10.

7. Anayol MA, Güler E, Yağci R, et al. Comparison of central corneal thickness, thinnest corneal thickness, anterior chamber depth, and simulated keratometry using Galilei, Pentacam, and Sirius devices. Cornea. 2014;33(6):582–6.

8. Shetty R, Arora V, Jayadev C, et al. Repeatability and agreement of three Scheimpflug-based imaging systems for measuring anterior segment parameters in keratoconus. Invest Ophthalmol Vis Sci. 2014;55(8):5263–8.

9. Shetty R, Rao H, Khamar P, et al. Keratoconus screening indices and their diagnostic ability to distinguish normal from ectatic corneas. Am J Ophthalmol. 2017;181:140–8.

10. Finis D, Ralla B, Karbe M, Borrelli M, Schrader S, Geerling G. Comparison of two different Scheimpflug devices in the detection of keratoconus, regular astigmatism, and healthy corneas. J Ophthalmol. 2015;2015: 315281.

11. Heidari Z, Hashemi H, Mohammadpour M, Amanzadeh K, Fotouhi A. Evaluation of corneal topographic, tomographic and biomechanical indices for detecting clinical and subclinical keratoconus: a comprehensive three-device study. Int J Ophthalmol. 2021;14(2):228–39.

12. Koh S, Ambrósio R Jr, Inoue R, Maeda N, Miki A, Nishida K. Detection of subclinical corneal ectasia using corneal tomographic and biomechanical assessments in a Japanese population. J Refract Surg. 2019;35(6):383–90.

13. Ambrósio R Jr, Caiado AL, Guerra FP, et al. Novel pachymetric parameters based on corneal tomography for diagnosing keratoconus. J Refract Surg. 2011;27(10):753–8.

14. Gharieb HM, Othman IS, Oreaba AH, Abdelatif MK. Topographic, elevation, and keratoconus indices for diagnosis of keratoconus by a combined Placido and Scheimpflug topography system. Eur J Ophthalmol. 2021;31(4):1553–62.

15. Feng K, Zhang Y, Chen YG. The possible causes for tomography suspect keratoconus in a Chinese cohort. BMC Ophthalmol. 2021;21(1):47.

16. Calossi A. Corneal asphericity and spherical aberration. J Refract Surg. 2007;23(5):505–14.

17. Ruiseñor Vázquez PR, Galletti JD, Minguez N, et al. Pentacam Scheimpflug tomography findings in topographically normal patients and subclinical keratoconus cases. Am J Ophthalmol. 2014;158(1):32–40.

18. Davis WR, Raasch TW, Mitchell GL, Mutti DO, Zadnik K. Corneal asphericity and apical curvature in children: a cross-sectional and longitudinal evaluation. Invest Ophthalmol Vis Sci. 2005;46(6):1899–906.

19. Hashemi H, Beiranvand A, Yekta A, Maleki A, Yazdani N, Khabazkhoob M. Pentacam top indices for diagnosing subclinical and definite keratoconus. J Curr Ophthalmol. 2016;28(1):21–6.

20. Arbelaez MC, Versaci F, Vestri G, Barboni P, Savini G. Use of a support vector machine for keratoconus and subclinical keratoconus detection by topographic and tomographic data. Ophthalmology. 2012;119(11):2231–8.

21. Gomes JA, Tan D, Rapuano CJ, et al. Global consensus on keratoconus and ectatic diseases. Cornea. 2015;34(4):359–69.

22. Moshirfar M, Motlagh MN, Murri MS, Momeni-Moghaddam H, Ronquillo YC, Hoopes PC. Galilei corneal tomography for screening of refractive surgery candidates: a review of the literature, Part II. Med Hypothesis Discov Innov Ophthalmol. 2019;8(3):204–18.